Experimental Determination of the Number of Trapped Ions, Detection Limit, and Dynamic Range in Fourier Transform Ion Cyclotron Resonance Mass Spectrometry

Patrick A. Limbach, Peter B. Grosshans,† and Alan G. Marshall*,‡

Department of Chemistry, 120 West 18th Avenue, The Ohio State University, Columbus, Ohio 43210

Determination of the number of ions that produce a detected time-domain signal in Fourier transform ion cyclotron resonance mass spectrometry is fundamental in establishing (a) the detection limit for a single data acquisition, (b) the maximum number of trapped ions, and (c) the mass spectral dynamic range obtained as the ratio of (b)/(a). Moreover, the ability to monitor ion absolute abundances throughout various experimental event sequences provides a direct measure of (e.g.) ionization efficiency, collisional-induced dissociation efficiency, and ion trapping efficiency. In this paper, we determine the absolute number of trapped ions by comparing the experimentally observed signal voltage to that calculated for a single ion orbiting at the (measured) ICR orbital radius of the ion packet, assuming that all ions orbit in a tight coherent packet in the trap midplane. The effects of relaxing these assumptions are estimated. In this way, we determine a detection limit (undamped signal acquired for 1 s, magnitude-mode mass spectral peak height to baseline standard deviation noise ratio of 3:1 measured at a frequency of 600 kHz, excited ICR orbital radius of 50% of the maximum possible cubic trap radius) of ~177 singly charged ions and a dynamic range of 32 000 at 3.0 T in a cubic trap. Various assumptions, the detection circuit model, and proposed applications for the determination of the number of trapped ions are discussed.

INTRODUCTION

Fourier transform ion cyclotron resonance mass spectrometry (FT/ICR/MS) has recently been combined with a very wide variety of analytically useful ionization techniques in which ions are initially formed outside the ion trap: e.g., laser desorption,[1] matrix-assisted laser desorption,[2] Cs^+ secondary ionization,[3,4] dc glow discharge,[5] electrospray,[6] fast neutral beam,[7] entrainment of ions in a supersonic jet,[8] continuous-flow fast atom bombardment,[9] supercritical fluid chromatography,[10] high-pressure ion source,[11] field desorption,[12] ^{252}Cf plasma desorption,[13] metal vapor vacuum arc,[14] and surface-induced dissociation.[15] The theoretical aspects of ion behavior in the ICR trap are now well understood, and recent advances in techniques for ion trapping and ICR excitation and detection have been comprehensively reviewed.[16,17] The groundwork is now in place for the increased use of FT/ICR/MS as a powerful analytical technique. With the rapid expansion in FT/ICR/MS analytical applications comes an increased need for a direct and accurate measure of the number of ions that contribute to the detected time-domain ICR signal, in particular the smallest and largest number of ions that may be detected.

The *minimum* detection limit for FT/ICR/MS is presently defined empirically as the minimum amount of sample which produces a specified mass spectral peak height-to-noise ratio under some sort of standard conditions.[18,19] However, such a definition represents a composite measure of the sample volatility, ionization efficiency, ion trapping efficiency, ion stability toward collisions or reactions, ICR orbital radius, trap size and shape, detection circuit equivalent resistance and capacitance, etc. In practice, these effects have not proved easy to separate, so that there is at present no good measure of the number of ions detected in an FT/ICR/MS experiment.

At the other end of the scale, it is important to establish the *maximum* number of detectable ions, in order to determine the *dynamic range* (ratio of largest to smallest observable signal in a single spectrum). Whereas the maximum number of ions that may be trapped can be estimated from space charge considerations,[20-22] the actual maximum number of

* To whom correspondence should be addressed.
† Present address: Analytical Sciences Lab, Corporate Research, Exxon Research & Engineering Co., Clinton Township, Rt. 22-East, Annandale, NJ 08801.
‡ Also a member of the Department of Biochemistry.

(1) *Lasers in Mass Spectrometry*; Lubman, D. M., Ed.; Oxford University Press: New York, 1990.
(2) Hettich, R. L.; Buchanan, M. V. *J. Am. Soc. Mass Spectrom.* **1991**, *2*, 22-28.
(3) Castro, M. E.; Russell, D. H. *Anal. Chem.* **1984**, *56*, 578-581.
(4) Amster, I. J.; Loo, J. A.; Furlong, J. J. P.; McLafferty, F. W. *Anal. Chem.* **1987**, *59*, 313-317.
(5) Barshick, C. M.; Eyler, J. R. *J. Am. Soc. Mass Spectrom.* **1992**, *3*, 122-127.
(6) Henry, K. D.; Williams, E. R.; Wang, B.-H.; McLafferty, F. W.; Shabanowitz, J.; Hunt, D. F. *Proc. Natl. Acad. Sci. U.S.A.* **1989**, *86*, 9075-9078.
(7) Hill, N. C.; Limbach, P. A.; Shomo, R. E., II; Marshall, A. G.; Appelhans, A. D.; Delmore, J. E. *Rev. Sci. Instrum.* **1991**, *62*, 2612-2617.
(8) Smalley, R. E. *Anal. Instrum.* **1988**, *17*, 1-21.
(9) Watson, C. H.; Kruppa, G.; Wronka, J.; Laukien, F. H. *Rapid Commun. Mass Spectrom.* **1991**, *5*, 249-251.
(10) Baumeister, E. R.; West, C. D.; Ijames, C. F.; Wilkins, C. L. *Anal. Chem.* **1991**, *63*, 251-255.
(11) Kofel, P.; McMahon, T. B. *Int. J. Mass Spectrom. Ion Processes* **1990**, *98*, 1-24.
(12) Ipezsa, I.; Knoll, H.; Wanczek, K.-P.; Linden, H. B. *Proceedings of the 36th American Society for Mass Spectrometry Annual Conference on Mass Spectrometry and Allied Topics*, San Francisco, CA, 1988; American Society for Mass Spectrometry: East Lansing, MI, 1988; pp 618-619.
(13) Williams, E. R.; McLafferty, F. W. *J. Am. Soc. Mass Spectrom.* **1990**, *1*, 427-430.
(14) Wang, B. H.; Amster, I. J.; McLafferty, F. W.; Brown, I. B. *Int. J. Mass Spectrom. Ion Processes* **1990**, *100*, 51-61.
(15) Ijames, C. F.; Wilkins, C. L. *Anal. Chem.* **1990**, *62*, 1295-1299.
(16) Marshall, A. G.; Grosshans, P. B. *Anal. Chem.* **1991**, *63*, 215A-229A.
(17) Marshall, A. G.; Schweikhard, L. *Int. J. Mass Spectrom. Ion Processes* **1992**, *118/119*, 37-70.
(18) Comisarow, M. B. In *Ion Cyclotron Resonance Spectrometry II*; Hartmann, H., Wanczek, K.-P., Eds.; Springer-Verlag: Berlin, 1982; pp 484-513.
(19) Sack, T. M.; McCrery, D. A.; Gross, M. L. *Anal. Chem.* **1985**, *57*, 1290-1295.
(20) Ledford, E. B., Jr.; Rempel, D. L.; Gross, M. L. *Anal. Chem.* **1984**, *56*, 2744-2748.
(21) Wang, T.-C. L.; Marshall, A. G. *Int. J. Mass Spectrom. Ion Processes* **1986**, *68*, 287-301.

0003-2700/93/0365-0135$04.00/0

trapped ions that contribute to the detected cyclotron signal is unknown.

Finally, a direct measure of the *absolute* number of ions contributing to the ICR signal is vital to such fundamental measurements as ionization efficiency, trapping efficiency (particularly for external ion injection), mechanisms for damping of the time-domain ICR signal, etc. Prior attempts to determine the number of detectable ions in an ICR ion trap include applying a dc voltage to one trapping plate to attract positive ions where the resultant ion current is measured with an electrometer;[23] calculating the number of ions of known electron ionization cross-section from measured electron beam duration, emission current, and ionization volume;[24,25] and applying a dc voltage to either the excitation or trapping electrodes of a cubic trap to induce ions to drift toward the detector electrodes, where their deposited charge is measured.[20,25] However, all of these methods at best determine the number of ions trapped *before* excitation and give no direct indication of the extent of ion loss or dephasing during and after the excitation process. In this paper, we offer a determination of ion number based directly on the observed ICR signal. We obtain the number of coherently orbiting ions simply by dividing the observed signal by the signal calculated for one ion at the same (measured) ICR orbital radius. The method requires only the (one-time) determination of the equivalent resistance and capacitance of the ICR trap and knowledge of the trap geometry. We begin by defining the detection limit and then proceed to review the theory and signal model for the method.

Detection Limit. In sector, quadrupole, and time-of-flight mass spectrometry, the preferred method of signal detection is simply ion counting,[26] so that determination of the detection limit is straightforward. In contrast, an FT/ICR mass spectrum is obtained from a time-domain voltage signal resulting from an image current induced by a coherently orbiting ion packet.[27-31] For an ionized sample containing ions of a single mass-to-charge ratio, m/q, the time-domain ICR signal is directly proportional to the number of ions. Thus, establishment of the absolute number of ions in an FT/ICR measurement requires four steps: (a) separation of the signals from ions of different m/q values; (b) determination of the proportionality factor between the number of ions of a given m/q and the observed voltage signal at their ICR orbital frequency; (c) determination of the noise level; (d) consideration of imprecision resulting from the discrete nature of the time-domain data. Separation of the signals from ions of different m/q is accomplished by discrete Fourier transformation to generate a frequency-domain spectrum.[32] Moreover, the theoretical nature[33,34] and experimental determination of FT/ICR mass spectral magnitude-mode noise are well-understood, as is the relation between spectral precision (in this case, with respect to mass spectral peak height or area) and the number of discrete data points per spectral peak width.[34-36] In this paper, we present the solution to the remaining step, (b), namely, determination of the voltage signal for a known number of ions orbiting in a coherent packet at a known ICR orbital radius.

A suitable definition of detection limit should be as independent as possible of instrumental parameters (e.g., type or size of ion trap, excitation amplitude or duration, and collisional damping of the time-domain ICR signal). Collisional damping may be minimized by choosing a data acquisition period that is short compared to the time-domain exponential damping time constant for the signal; FT/ICR mass spectral peak width is then a function only of acquisition period.[37] On the other hand, since frequency-domain signal-to-noise ratio increases as the square root of acquisition period,[37] the acquisition period should be as long as possible, consistent with the need to avoid signal damping as noted above. As a compromise, we suggest a 1-s acquisition period, at which the time-domain signal should remain undamped at the readily attainable sample pressure of $\sim 10^{-9}$ Torr. ICR time-domain signal strength increases approximately proportional to ICR orbital radius;[29,31,38] however, nonlinear effects introduce complications as the ICR orbital radius approaches the detection electrodes. Again, as a working compromise, we suggest a standard ICR orbital radius equal to half the maximum radius of the trap [e.g., half the inner radius of the ring electrode for cylindrical or hyperbolic traps or half the (lesser of the) excitation or detection plate-to-plate separation in an orthorhombic trap]. Finally, the signal-to-noise ratio should be measured from the frequency-domain FT spectrum, not the time-domain signal, because only the FT spectrum separates signals from ions of different m/q values. The above criteria may be summarized in the following definition of detection limit for FT/ICR mass spectrometry. *The detection limit of an FT/ICR/MS instrument is the minimum number of ions, in a single scan, required to produce a signal whose FT magnitude-mode peak height is 3 times the noise level (defined as the standard deviation of the magnitude-mode baseline noise) for a 1-s observation period of an ICR time-domain signal whose exponential decay time constant is at least 10 s (i.e., negligible signal damping during the detection period), for ions at an initial average postexcitation ICR orbital radius of half the maximum allowed radius.* Because the signal-to-noise ratio in FT/ICR/MS may depend on frequency,[27] we have specified 600 kHz (ion cyclotron orbital frequency to the benzene molecular ion at 3.0 T) as a reference frequency.

Dynamic Range. The dynamic range of FT/ICR mass spectrometry has been variously estimated to be in the 10^3–10^5 range for a single time-domain data acquisition,[23,24] with substantial extension by use of stored-waveform selective ejection of the ions of highest relative abundance.[39] Knowledge of the dynamic range is obviously important for detecting minor constituents in a spectrum. However, present estimates

(22) Ledford, E. B., Jr.; Rempel, D. L.; Gross, M. L. *Anal. Chem.* **1984**, *56*, 2744–2748.
(23) Hunter, R. L.; Sherman, M. G.; McIver, R. T., Jr. *Int. J. Mass Spectrom. Ion Phys.* **1983**, *50*, 259–274.
(24) McIver, R. T., Jr.; Hunter, R. L.; Ledford, E. B., Jr.; Locke, M. J.; Francl, T. J. *Int. J. Mass Spectrom. Ion Phys.* **1981**, *39*, 65.
(25) Elling, J. W.; Farrar, T. C.; Campana, J. E. *Proceedings of the 39th American Society for Spectrometry Annual Conference on Mass Spectrometry and Allied Topics*, Nashville, TN, 1991; American Society for Mass Spectrometry: East Lansing, MI, 1991; pp 457–458.
(26) White, F. A.; Wood, G. A. *Mass Spectrometry Applications in Science and Engineering*; John Wiley & Sons: New York, 1986, Chapter 5.
(27) Comisarow, M. B. *J. Chem. Phys.* **1978**, *69*, 4097–4104.
(28) Marshall, A. G.; Wang, T.-C. L.; Cottrell, C. E.; Werbelow, L. G. *J. Am. Chem. Soc.* **1982**, *104*, 7665–7666.
(29) Rempel, D. L.; Huang, S. K.; Gross, M. L. *Int. J. Mass Spectrom. Ion Processes* **1986**, *70*, 163–184.
(30) Nikolaev, E. N.; Gorshkov, M. V. *Int. J. Mass Spectrom. Ion Processes* **1985**, *64*, 115–125.
(31) Grosshans, P. B.; Shields, P. J.; Marshall, A. G. *J. Chem. Phys.* **1991**, *94*, 5341–5352.
(32) Marshall, A. G.; Verdun, F. R. *Fourier Transforms in NMR, Optical, and Mass Spectrometry: A User's Handbook*; Elsevier: Amsterdam, 1990; 460 pp.
(33) Hanna, D. A. *Proceedings of the 33rd American Society for Mass Spectrometry Annual Conference on Mass Spectrometry and Allied Topics*, San Diego, CA, 1985; American Society for Mass Spectrometry: East Lansing, MI, 1985; pp 435–436.
(34) Liang, Z.; Marshall, A. G. *Appl. Spectrosc.* **1990**, *44*, 766–775.
(35) Chen, L.; Cottrell, C. E.; Marshall, A. G. *Chemom. Intell. Lab. Syst.* **1986**, *1*, 51–58.
(36) Liang, Z.; Marshall, A. G. *Anal. Chem.* **1990**, *62*, 70–75.
(37) Marshall, A. G. *Anal. Chem.* **1979**, *51*, 1710–1714.
(38) Grosshans, P. B.; Marshall, A. G. *Int. J. Mass Spectrom. Ion Processes* **1990**, *100*, 347–379.
(39) Wang, T.-C. L.; Ricca, T. L.; Marshall, A. G. *Anal. Chem.* **1986**, *58*, 2935–2938.

of dynamic range suffer from lack of knowledge both of the maximum number of detectable ions and of the detection limit (see above). For example, even if a large number of ions can be trapped, space charge (Coulomb repulsion) effects may tend to spread them out in the trap, reducing the coherence of the excited ICR signal and resulting in axial and radial ion loss as well as loss of signal due to charge induced on the trap electrodes rather than the detector electrodes.

Dynamic range in FT/ICR experiments is limited by both *analog* and *digital* stages. Digital dynamic range is limited (for a single data acquisition of a noiseless signal) by the word length in the analog-to-digital conversion (ADC) step. For typical 10–12-bit ADC's used for FT/ICR/MS, the digital dynamic range per acquisition is thus limited to 1000–4000. Dynamic range may exceed the number of bits per ADC word by use of signal-averaging[32] of multiple acquisitions of noisy signals (e.g., electron ionization), because the signal accumulates as the number of acquisitions whereas the noise accumulates only as the square root of the number of acquisitions.[37] Thus, we shall here be concerned mainly with *analog* dynamic range for a signal accumulated for many acquisitions.

THEORY

Detection Circuit Model. The general theory of detection in the FT/ICR experiment has been described previously.[27,29-31] The detection circuit is shown in Figure 1. A coherently orbiting ion packet induces a differential signal current between the receiver plates and can be modeled as a current source (S in Figure 1). The receiver plates may be modeled as an equivalent capacitor (C in Figure 1) and resistor (R in Figure 1) in parallel which pass this charge to the preamplifier depending on the frequency of the induced charge. To this point, we have followed Comisarow's prior treatment.[27]

In the interest of simplicity and in an effort to draw a parallel with NMR, Comisarow formulated his theory in terms of a dipole moment per unit volume, P, which, generally speaking, does not apply to localized gas-phase ions interacting with finite-dimension receiver electrodes. The Comisarow model gives a correct result for infinite parallel plate receiver electrodes and a symmetrical charge distribution but fails to account for a number of other effects. A consequence of the model is that the induced surface charge density on the detection plates is independent of position. In fact, the surface charge density varies with position.[31] The Comisarow model also neglects dependence of signal on ion axial position, fails to account for harmonic signals, and predicts a linear (rather than approximately linear, reduced by a factor of 0.721 67 for a cubic trap) dependence of ICR signal on ICR orbital radius.[31] Finally, the original Comisarow treatment does not apply to geometries/detection circuits in which even harmonics do not cancel by symmetry (e.g., single-electrode detection[40]) or where magnetron/trapping motion is present (as in all actual ICR ion traps). The more recent model on which the present development is based[31] accommodates all of the above issues. To determine the induced charge on the receiver plates, we therefore proceed as follows:

Let a charge source S induce a differential charge, ΔQ, between the two detect electrodes. The induced charge can be expanded in a Fourier series with coefficients $[A_{2m+1}(2r/a)$, scaled according to the trap geometry] corresponding to the amplitude of the induced charge component at each odd integral multiple ($m = 0, 1, 2, ...$) of the ICR orbital frequency, ω_+, in which r is the ICR orbital radius and a is the distance between the centers of the two detector electrodes. Specifically

$$-\Delta Q/q = \sum_{m=0}^{\infty} A_{2m+1}(2r/a) \cos [(2m+1)\omega_+ t] \quad (1)$$

or

$$\Delta Q = -q \sum_{m=0}^{\infty} A_{2m+1}(2r/a) \cos [(2m+1)\omega_+ t] \quad (2)$$

Since electrical current, $i(t)$, is simply the time rate of change of (induced) charge on the detector electrode(s)

$$i(t) = \frac{d}{dt}\frac{\Delta Q}{2} = \frac{d}{dt}\left[\frac{-q}{2}\sum_{m=0}^{\infty} A_{2m+1}\left(\frac{2r}{a}\right) \cos [(2m+1)\omega_+ t]\right] \quad (3)$$

The factor of $^1/_2$ on the right-hand side of eq 3 is introduced to avoid counting the current twice (once for current flowing out of one detector plate and once for current flowing into the other detector plate). Since current flows either through the resistor [$i(t) = V(t)/R$] or through the capacitor [$i(t) = C\mathrm{d}V(t)/\mathrm{d}t$] of the equivalent circuit of Figure 1[27]

$$i(t) = C\left[\frac{V(t)}{RC} + \frac{dV(t)}{dt}\right] \quad (4)$$

in which $V(t)$ is the differential voltage corresponding to the induced differential charge, ΔQ, and R is resistance. Multiplying eq 4 by $\exp(t/RC)$ to create an exact differential, we obtain

$$i(t) = \exp(-t/RC)C\frac{d}{dt}(\exp(t/RC)V(t)) \quad (5)$$

so that

$$\frac{q\omega_+}{2C}\sum_{m=0}^{\infty}(2m+1)A_{2m+1}\left(\frac{2r}{a}\right)\exp(t/RC)\sin[(2m+1)\omega_+ t] = \frac{d}{dt}(\exp(t/RC)V(t)) \quad (6)$$

or

$$\frac{q\omega_+}{2C}\sum_{m=0}^{\infty}(2m+1)A_{2m+1}\left(\frac{2r}{a}\right)\int_{-\infty}^{t}\sin[(2m+1)\omega_+ t'] \exp(t'/RC)\,dt' = \exp(t/RC)V(t) \quad (7)$$

$$\frac{V(t)}{\frac{q\omega_+}{2C}} = \exp(-t/RC)\sum_{m=0}^{\infty}(2m+1)A_{2m+1}\left(\frac{2r}{a}\right)\times \left\{\left[\exp(t'/RC)\frac{1}{RC}\sin[(2m+1)\omega_+ t'] - (2m+1)\omega_+ \cos[(2m+1)\omega_+ t']\right]/\left[\frac{1}{R^2C^2} + (2m+1)^2\omega_+^2\right]\right\}\Bigg|_{-\infty}^{t} \quad (8)$$

$$V(t) = \frac{q\omega_+ R}{2}\sum_{m=0}^{\infty}(2m+1)A_{2m+1}(\bar{r})\times \{[\sin[(2m+1)\omega_+ t] - (2m+1)RC\omega_+ \cos[(2m+1)\omega_+ t]]/[1 + [(2m+1)\omega_+ RC]^2]\} \quad (9)$$

in which $\bar{r} = r/(a/2)$ = the ICR orbital radius measured as a fraction of the radius from the center of the trap to the center of either detector electrode. In order to exploit the trigonometric identity, $\sin A \cos B - \cos A \sin B = \sin(A - B)$, we find it useful to define $\theta_m = \tan^{-1}[(2m+1)\omega_+ RC]$, so that

(40) Allemann, M.; Kellerhals, H.-P.; Wanczek, K.-P. *Chem. Phys. Lett.* **1981**, *84*, 547–551.

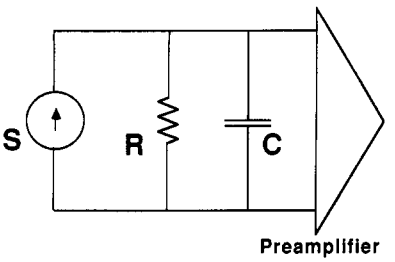

Figure 1. Diagram of the equivalent circuit representation of the detection model used in this paper: signal current source (S), detection circuit equivalent capacitance (C) and resistance (R), and preamplifier. The signal model of this figure is equivalent to a prior model for differential detection.[27]

$$V(t) = \frac{q\omega_+R}{2}\sum_{m=0}^{\infty}\frac{(2m+1)A_{2m+1}(\bar{r})}{\sqrt{1+[(2m+1)RC\omega_+]^2}}\sin[(2m+1)\omega_+ - \theta_m] \quad (10)$$

or

$$V(t) = \frac{q}{2C}\sum_{m=0}^{\infty}A_{2m+1}(\bar{r})\sin(\theta_m)\sin[(2m+1)\omega_+t - \theta_m] \quad (11)$$

Keeping only the first term of the sum in eq 11 (i.e., neglecting third and higher-order harmonic signal components), we arrive at

$$V(t) \approx \frac{q}{2C}A_1(\bar{r})\sin(\theta_0)\sin[\omega_+t - \theta_0] \quad (12)$$

$$V(t) = \frac{q}{2C}A_1(\bar{r})\frac{\omega_+RC}{\sqrt{1+(\omega_+RC)^2}}\sin[\omega_+t - \theta_0] \quad (13)$$

For $\omega_+RC \gg 1$ (i.e., for $R \approx 1$ MΩ and $C \approx 40$ pf, $m/q \leq 4000$ u/e at 3.0 T) and

$$\theta_0 = \tan^{-1}[\omega_+RC] \approx \pi/2 \quad (14)$$

$$V(t) \approx \frac{q}{2C}A_1(\bar{r})\cos(\omega_+t) \quad (15)$$

Equation 15 gives the voltage signal for a single ion. For N identical ions of charge q

$$V(t) = \frac{Nq}{2C}A_1(\bar{r})\cos(\omega_+t) \quad (16)$$

or

$$N = 2CV(t)/qA_1(\bar{r})\cos(\omega_+t) \quad (17)$$

$$N = 2C\frac{V_{p\text{-}p}}{2}/qA_1(\bar{r}) \quad (18)$$

$$N = CV_{p\text{-}p}/qA_1(\bar{r}) \quad (19)$$

In order to determine the number of ions contributing to the detected signal, the capacitance, C, of the detection circuit must be determined, the peak-to-peak voltage corresponding to a measured FT/ICR mass spectral peak amplitude must be known, and the radius, r, must be determined. $A_1(\bar{r})$, which is approximately proportional to $\bar{r}$, may be determined graphically.[38] The capacitance of the detection circuit and the calibration of the peak-to-peak voltage/spectral peak amplitude may both be determined once for a given instrument. The radius determination has been described previously.[41]

Signal-to-Noise Ratio. If the noise is modeled as a detection-limited (Johnson) noise source and amplifier noise is neglected,[42] then the time-domain rms noise voltage, V_{noise}, takes the form

$$V_{noise} = \sqrt{\frac{4kT\delta\omega/R}{1+(\omega_+RC)^2}} \quad (20)$$

in which $\Delta\omega$ is the detection bandwidth, T is absolute temperature, and k is Boltzmann's constant. From eqs 13 and 20, the ratio of the signal peak-to-peak amplitude-to-noise ratio then becomes

$$V_{peak\text{-}to\text{-}peak\ signal}/V_{noise} = NqA_1(\bar{r})\omega_+R/4\sqrt{kT\delta\omega/R} \quad (21)$$

independent of whether the detection circuit is predominantly capacitive (i.e., $\omega_+RC \gg 1$) or predominantly resistive ($\omega_+RC \ll 1$): in the capacitive limit, the signal is independent of frequency whereas the noise varies inversely with frequency; in the resistive limit, the signal varies directly with frequency and the noise is independent of frequency. Equation 21 shows that the signal-to-noise ratio is frequency-dependent; thus, any definition of the detection limit must account for that frequency dependence. Equation 21 also shows that signal-to-noise ratio is proportional to ICR orbital frequency (and thus to magnetic field strength).

Note that eq 21 is valid only if the noise is dominated by Johnson noise. In that case, the current noise is frequency-independent, but the voltage noise (in the capacitive limit) varies inversely with frequency. Experimentally, except at quite low ICR frequency (<10 kHz), predominantly capacitive detection circuits typically yield frequency-independent voltage noise.[18] In that case, the present method for determining the number of ions remains valid, and signal-to-noise ratio is independent of ICR frequency. Finally, at sufficiently low frequency, detection becomes predominantly resistive (i.e., $\omega_+RC \ll 1$), and the signal varies directly with frequency. Thus, signal-to-noise ratio is expected to be independent of frequency both at high frequency (predominantly capacitive detection, voltage noise independent of frequency) and at very low frequency (predominantly resistive detection, Johnson noise dominant).

EXPERIMENTAL SECTION

Detection Circuit Capacitance. The capacitance calibration was performed by leaking benzene (at a pressure of 5×10^{-7} Torr measured on the source trap ion gauge) into the vacuum chamber. A variable-capacitance bridge was designed and inserted in parallel to the detection circuit. A variety of capacitors was added to the capacitance bridge for each experiment, and the FT/ICR magnitude-mode peak height for the molecular ion of benzene was determined by three-point quadratic interpolation. The conventional experimental event sequence was employed: trap quenching for 1 ms to remove ions, electron beam duration of 500 μs at an emission current of 4.38 μA (measured just behind the electron filament) to form new ions, single-frequency on-resonance excitation (24 $V_{p\text{-}p}$), and direct-mode broad-band detection (4K data points, 2-MHz bandwidth). Each time-domain signal was padded with 15 × 4K zeroes before fast Fourier transformation and magnitude calculation. The event sequence was repeated 2000 times to acquire a spectrum with a magnitude-mode spectral peak height-to-noise ratio of ~25:1.

Signal Level Calibration. To determine the signal level from a known voltage source, a frequency generator was added in parallel to the trap at the detection preamplifier. The experi-

(41) Grosshans, P. B.; Marshall, A. G. *Int. J. Mass Spectrom. Ion Processes* **1992**, *115*, 1–19.
(42) Comisarow, M. B. *Int. J. Mass Spectrom. Ion Phys.* **1981**, *37*, 251–257.

mental event sequence was the same as for the trap cross capacitance measurements except that single transients were recorded and the excitation was broadband (although single-frequency excitation could as easily be used). Single-scan magnitude-mode spectral peak heights were measured as described above as a function of the input voltage at various frequencies to determine the response of the preamplifier over the detection bandwidth. The rf voltage of the input from the frequency generator was attenuated to 181.8, 90.90, 19.80, and 9.901 μV_{p-p} for the input voltage level. The signal amplification was set to ×1, ×10, and ×100 for each of the frequencies and voltages investigated to determine the linearity of the analog-to-digital converter amplifier and its effects on the detected peak heights.

Ion Cyclotron Orbital Radius Determination. The average ion cyclotron orbital radius of the ion packet was found by measuring the magnitude ratio of the $C_6H_6^+$ signal at the third harmonic to that at the fundamental ICR orbital frequency. The experimental event sequence consisted of quench period; formation of the ions at 25-V electron beam energy at 4.32-μA emission current, 10-ms electron beam duration; single-frequency on-resonance excitation (14-V_{p-p} excitation amplitude) for 500 μs; 100-ms delay; broad-band detection (4K data points, 2-MHz bandwidth). For each measurement, 100 scans were coadded, padded with 15 × 4K zeroes, apodized with a Blackman-Harris apodization function, fast Fourier transformed, and displayed in magnitude mode. The magnitudes of the signals at the third and first harmonic frequencies were determined from their respective magnitude-mode FT/ICR mass spectral peak heights.[43] Because first and third harmonic signals may decay exponentially at different rates,[44] we set the time-domain acquisition period to be short compared to the exponential damping time constant, so that the frequency-domain relative areas of the two peaks[36] could be well-approximated by the relative frequency-domain peak heights at the first and third harmonic frequencies. The ICR orbital radius was then determined from the ratio of the third-to-first harmonic signal peak heights as described previously.[41,45] The measurement was performed five times, and the average ICR orbital radius was found to be 57% of the maximum allowed trap radius.

Ion Number Determination: Detection Limit. The number of ions contributing to the detected signal was determined as follows. All experiments were performed in heterodyne detection mode, with single-frequency excitation (14 V_{p-p}) for 500 μs and a detection period of 1 s. The number of trapped ions was varied by changing the gas pressure at constant electron beam duration (10 ms) and emission current (4.32 μA). The gas pressure at the source side of the dual trap was held to less than 2×10^{-8} Torr to ensure that the signal remained constant (i.e., undamped) throughout the detection period. Peak heights were measured exactly as before, and the noise level was determined from a software command which fits magnitude-mode baseline noise to a Rayleigh distribution histogram, for a signal-free baseline segment.[33] The noise level is reported as the standard deviation of magnitude-mode baseline noise, which is half the magnitude-mode root-mean-square baseline noise.[46] The signal level is reported as the maximum interpolated magnitude-mode peak height, based on a three-point quadratic fit to the largest three data points per peak. The above-determined signal and noise then define the experimental signal-to-noise ratio for each experiment.

RESULTS AND DISCUSSION

Calibration of the Detection Circuit Capacitance. The detection circuit capacitance arises from the coaxial feedthroughs to and from the trap, the detection plates, and the preamplifier circuit. To obtain a measurement of this capacitance, we added known capacitors to the capacitance bridge and measured the magnitude-mode FT/ICR mass spectral peak height. Because the capacitance bridge was inserted in parallel to the detection circuit, the data should follow the functional form

$$C_x = \frac{\text{constant}}{\text{ion signal}} - C_0 \qquad (22)$$

in which C_x is the measured capacitance with the capacitance bridge inserted into the detection circuit, the ion signal magnitude is determined by the software (see Experimental Section), and C_0 is the capacitance of the detection circuit. From eq 22, it is clear that the ICR signal decreases as capacitance, C_x, is added to the detection circuit. Thus, the y intercept of a plot of $(\text{signal})^{-1}$ vs the measured capacitance, C_x, yields C_0 = 51.7 pF. That value was then used in all subsequent calculations of the number of ions from a given detected signal voltage. The error in the measurement of the detection circuit capacitance is ~±10%, as determined by multiple measurements under identical conditions and statistical analysis of the linear least squares fit of eq 22.

Calibration of the Detector Response to a Known Signal Level Input. The calibration of the detection circuit to a known voltage input was performed at a variety of frequencies for several amplification levels and for several input voltages (see Experimental Section). The calibration curves at 500 kHz (not shown) for ×1, ×10, and ×100 amplification were fitted to straight lines with slightly different slopes:

$$\text{voltage} = 4.23 \times 10^{-5}(\text{magnitude-mode peak max}) \quad (\times 1 \text{ amplification}) \qquad (23)$$

$$\text{voltage} = 4.20 \times 10^{-6}(\text{magnitude-mode peak max}) \quad (\times 10 \text{ amplification}) \qquad (24)$$

$$\text{voltage} = 4.35 \times 10^{-7}(\text{magnitude-mode peak max}) \quad (\times 100 \text{ amplification}) \qquad (25)$$

The generally good agreement between these values indicates that the amplifier chain is essentially linear for this instrument. The slopes from eqs 23–25 were then used to determine the signal voltage in the following three sections.

Detection Limit. Equation 19 gives the formula for calculating the number of ions in a detected signal. The ion cyclotron orbital radius and trap cross capacitance are determined as noted above. The calibration curve of the previous section allows for the determination of the voltage level. The resulting detection limit is shown in Figure 2, in which we plot the number of detected ions as a function of the observed magnitude-mode spectral peak height-to-noise ratio. The data are described by

$$\text{no. of ions} = 59(\text{signal-to-noise ratio}) \qquad (26)$$

Extrapolating to a signal-to-noise ratio of 3:1, we find that the detection limit defined as the number of singly charged ions that produce this signal-to-noise ratio is ~177 for a 1-s time-domain data acquisition period.

Equation 16 is based on the assumption that the induced differential signal voltage arises from a point charge centered on the z-axis of the trap. If ions are in fact distributed along the z-axis, then the actual number of trapped ions will be higher than the above-listed estimate, since the induced signal voltage decreases with increasing z-distance away from the trap center.[47] Thus, the stated detection limit of ~177 singly-charged ions represents a *minimum* number of detectable

(43) Serreqi, A.; Comisarow, M. B. *Appl. Spectrosc.* **1987**, *41*, 288–295.
(44) Grosshans, P. B.; Marshall, A. G. *Int. J. Mass Spectrom. Ion Processes* **1991**, *107*, 49–81.
(45) Grosshans, P. B.; Shields, P. J.; Marshall, A. G. *J. Am. Chem. Soc.* **1990**, *112*, 1275–1277.
(46) Williams, C. P.; Marshall, A. G. *Anal. Chem.* **1992**, *64*, 916–923.
(47) Chen, R.; Grosshans, P. B.; Marshall, A. G. Unpublished results, 1992.

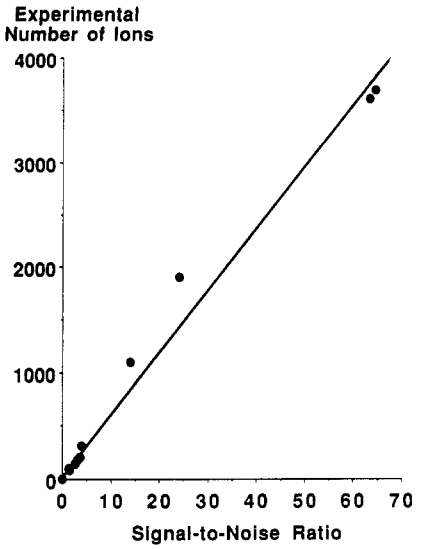

Figure 2. Plot of number of $C_6H_6^+$ ions at 3.0 T (~600-kHz ICR orbital frequency) contributing to the detected signal as a function of FT/ICR/MS magnitude-mode signal-to-noise ratio. Extrapolated to a magnitude-mode peak height-to-baseline standard deviation noise ratio of 3:1; the detection limit is 177 ions, for a 1-s detection period for ions excited to half their maximum possible ion cyclotron orbital radius in a 1.875-in.-diameter cubic trap.

trapped ions in a 1.875-in. cubic trap at an ion cyclotron orbital frequency of 600 kHz.

Maximum Number of Ions and Dynamic Range. The maximum number of detected trapped ions at various trapping voltages is shown in Figure 3. Under the ionization conditions for these experiments, the number of trapped ions reaches a maximum at ≥2-V trapping potential (1.875-in.

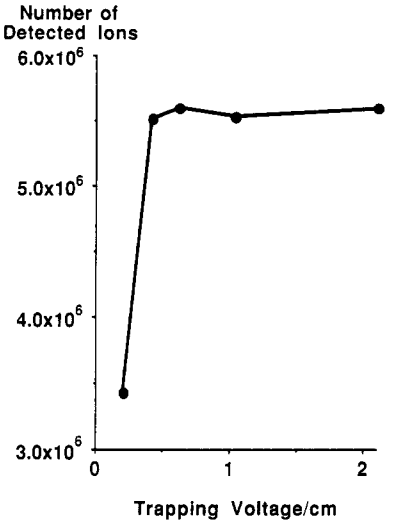

Figure 3. Plot of the maximum number of $C_6H_6^+$ ions that can be detected as a function of trapping voltage. Note that the maximum ion number is constant at ~5.6 × 10^6 over a trapping voltage range of 0–2 V/cm. The ratio of the maximum number of trapped ions (Figure 3) to the detection limit (Figure 2) yields a dynamic range of ~32 000:1.

separation between trapping electrodes). The maximum number of trapped ions is ~5.6 × 10^6 ions. From that number and the detection limit of ~177 ions, the dynamic range of the technique is ~3.2 × 10^4. Of course, a large number of ions leads to space charge effects[22,48,49] such as Coulomb broadening of the peaks,[50–52] but in some applications it may be desirable to trap as many ions as possible when bulk samples that have minor constituents are analyzed. The number of trapped ions may be increased by elongating,[23] screening,[53] or widening the trap or by use of parametric excitation/detection[54] of ions initially formed off-axis. Minor constituent ion abundances may also be built up by ejecting all unwanted species by SWIFT[55,56] or other multiple resonance techniques.

Multiply-Charged Ions. The induced ICR signal magnitude is proportional to the number of charges per ion. Therefore, in light of the recent electrospray FT/ICR/MS work by several research groups[6,57,58] on multiply-charged proteins, it is interesting to note that the detection limit for a signal-to-noise ratio of 3:1 for a detection period of 1 s reduces to just 9 ions which carry ±20 elementary charges. Thus, FT/ICR/MS sensitivity for electrosprayed ions approaches single-ion detectability.

ACKNOWLEDGMENT

This work was supported by grants (to A.G.M.) from the National Science Foundation (CHE-90-21058) and The Ohio State University.

RECEIVED for review March 5, 1992. Accepted October 5, 1992.

(48) Jeffries, J. B.; Barlow, S. E.; Dunn, G. H. *Int. J. Mass Spectrom. Ion Processes* **1983**, *54*, 169–187.
(49) Rempel, D. L.; Grese, R. P.; Gross, M. L. *Int. J. Mass Spectrom. Ion Processes* **1990**, *100*, 381–395.
(50) Chen, S.-P.; Comisarow, M. B. *Rapid Commun. Mass Spectrom.* **1991**, *5*, 450–455.
(51) Chen, S.-P.; Comisarow, M. B. *Rapid Commun. Mass Spectrom.* **1992**, *6*, 1–3.
(52) Hendrickson, C. L.; Beu, S. C.; Laude, D. A., Jr. *Proceedings of the 40th American Society for Mass Spectrometry Annual Conference on Mass Spectrometry and Allied Topics*, Washington, DC, 1992; American Society for Mass Spectrometry: East Lansing, MI, 1992; pp 723–724.
(53) Wang, M.; Marshall, A. G. *Anal. Chem.* **1989**, *61*, 1288–1293.
(54) Rempel, D. L.; Ledford, E. B., Jr.; Huang, S. K.; Gross, M. L. *Anal. Chem.* **1987**, *59*, 2527–2532.
(55) Marshall, A. G.; Wang, T.-C. L.; Ricca, T. L. *J. Am. Chem. Soc.* **1985**, *107*, 7893–7897.
(56) Marshall, A. G.; Wang, T.-C. L.; Chen, L.; Ricca, T. L. In *ACS Symposium Series*; Buchanan, M. V., Ed.; American Chemical Society: Washington, DC, 1987; Vol. 359, pp 21–33.
(57) Henry, K. D.; Quinn, J. P.; McLafferty, F. W. *J. Am. Chem. Soc.* **1991**, *113*, 5447–5449.
(58) Hofstadler, S. A.; Laude, D. A., Jr. *Proceedings of the 39th American Society for Mass Spectrometry Annual Conference on Mass Spectrometry and Allied Topics*, Nashville, TN, 1991; American Society for Mass Spectrometry: East Lansing, MI, 1991; pp 1538–1539.